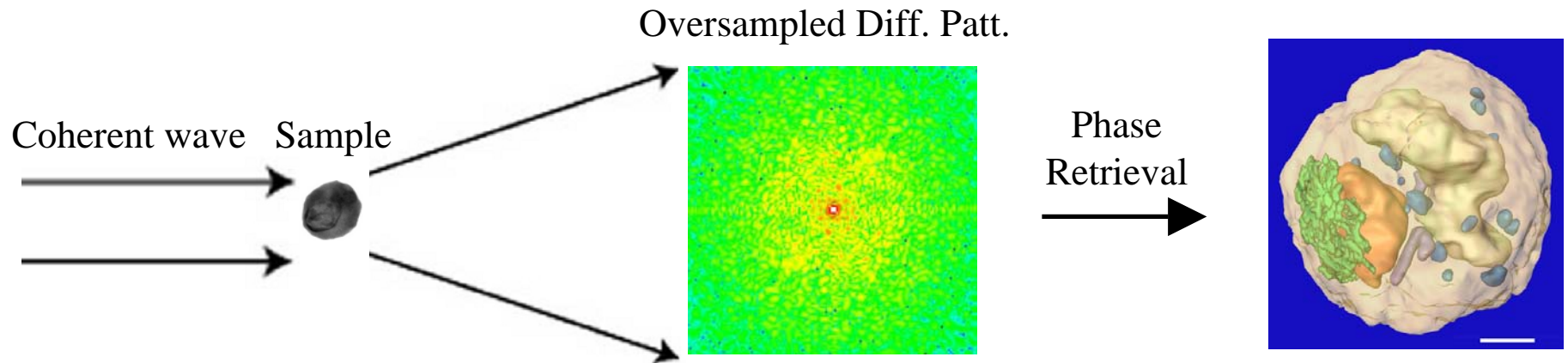

Ankylography: Three-Dimensional Structure Determination from a Single View

Jianwei (John) Miao

*Dept. of Physics and Astronomy &
California NanoSystems Institute, UCLA*

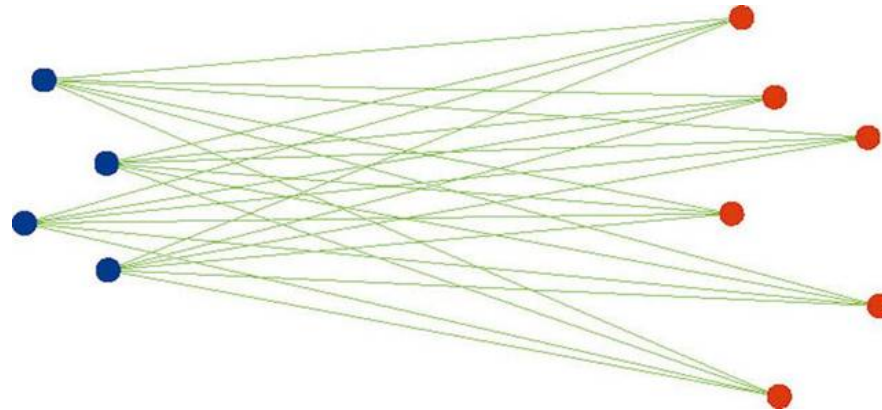
KITP Conference on X-ray Science in the 21st Century
UCSB, Aug. 2-6, 2010

Foundation of Coherent Diffractive (Lensless) Imaging



Real Space

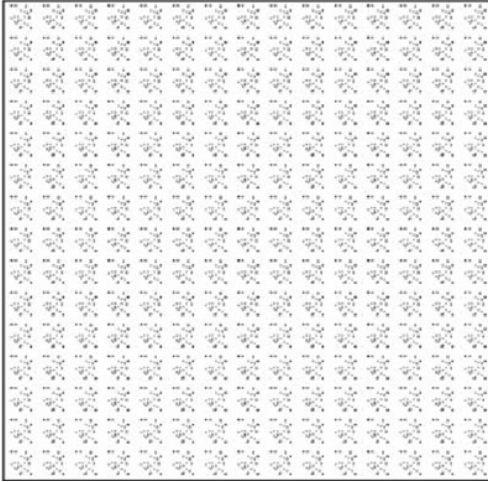
Reciprocal Space



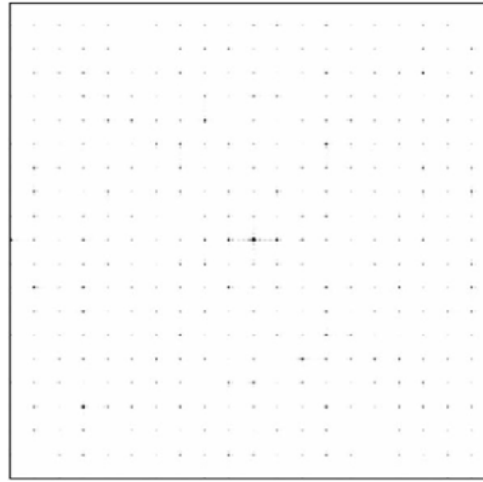
**Coherence \Rightarrow Oversampled intensity points that are correlated
 \Rightarrow Iterative algorithm \Rightarrow Phases**

Miao, Ishikawa, Johnson, Anderson, Lai & Hodgson, *PRL* **89**, 088303 (2002).

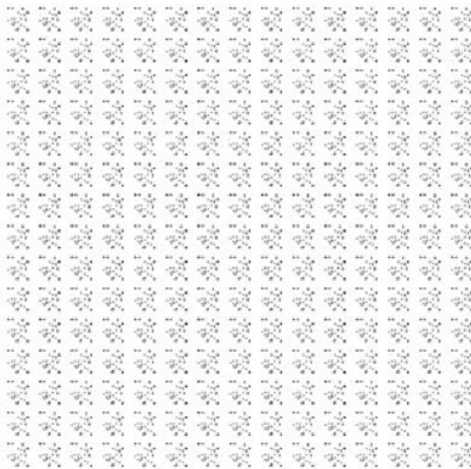
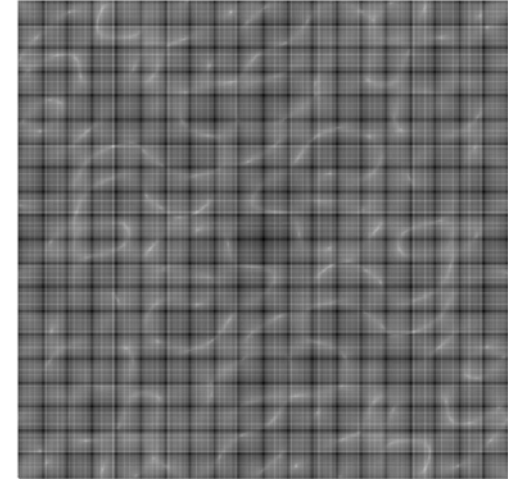
Coherence Length > the Size of a Nanocrystal



A nanocrystal consisting of 15 x 15 unit cells



Oversampled diffraction pattern in a linear and logarithmic scales



The reconstructed nanocrystal

“..., the phase information could be recovered from computer-generated oversampled diffraction patterns of small specimens that are (a) perfect or imperfect crystals, or (b) have a repeated motif without orientational regularity, or (c) are an unrepeated motif, such as an amorphous glass, a single molecule or a single biological cell.”

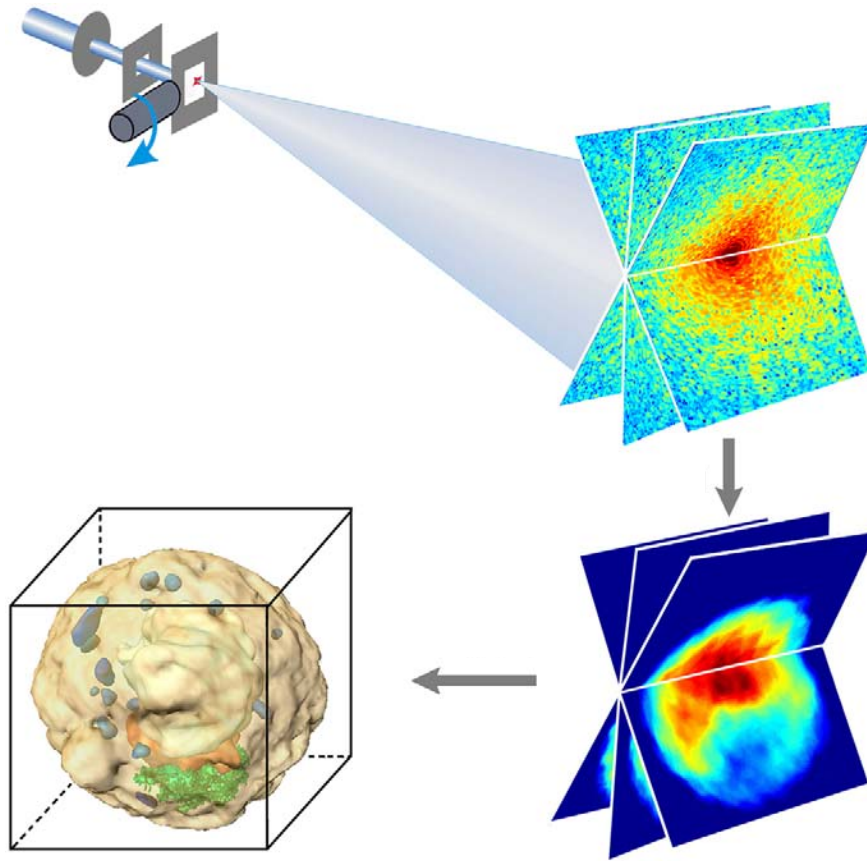
Miao & Sayre, *Acta Cryst. A* **56**, 596-605 (2000).

Current 3D Structure Determination Techniques

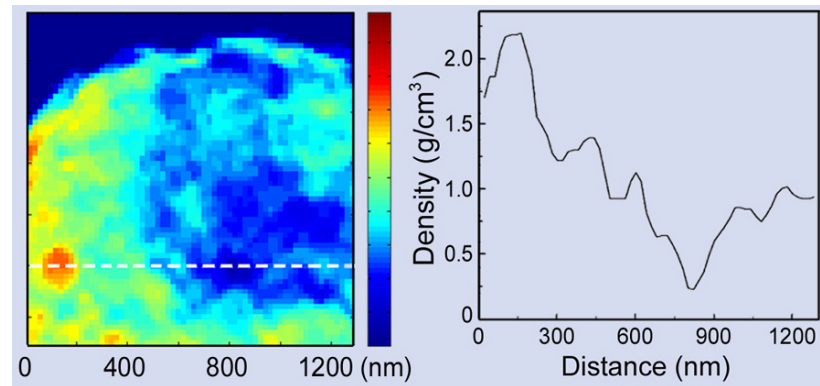
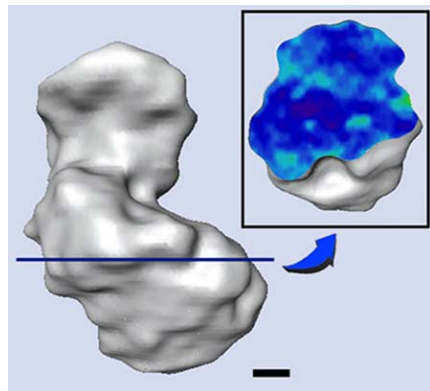
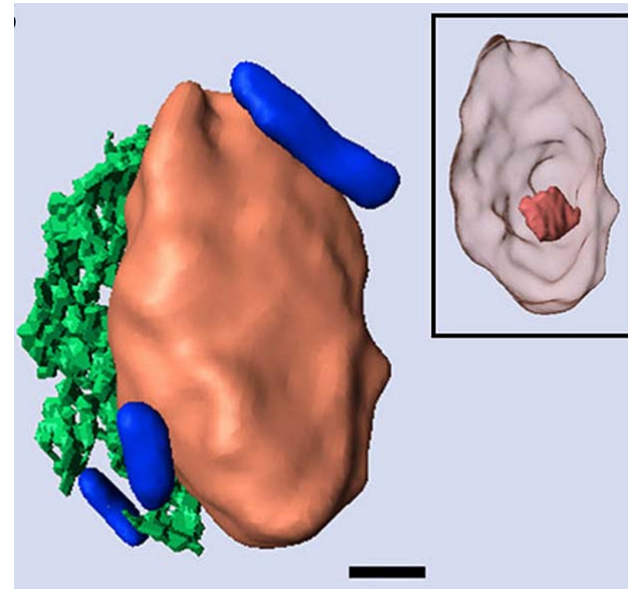
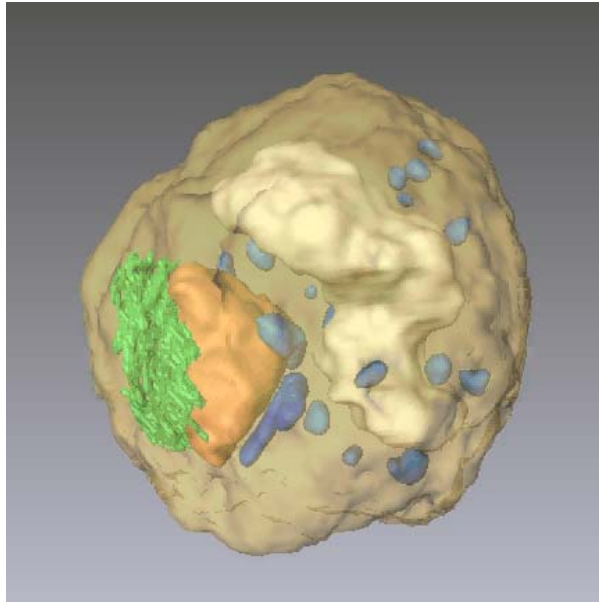
Crystallography, Tomography, 3D Coherent Diffractive Imaging:

Acquiring multiple measurements at various sample orientations.

Confocal microscopy: Scanning a series of thin sections through a sample.



Quantitative 3D Imaging of a Yeast Spore Cell



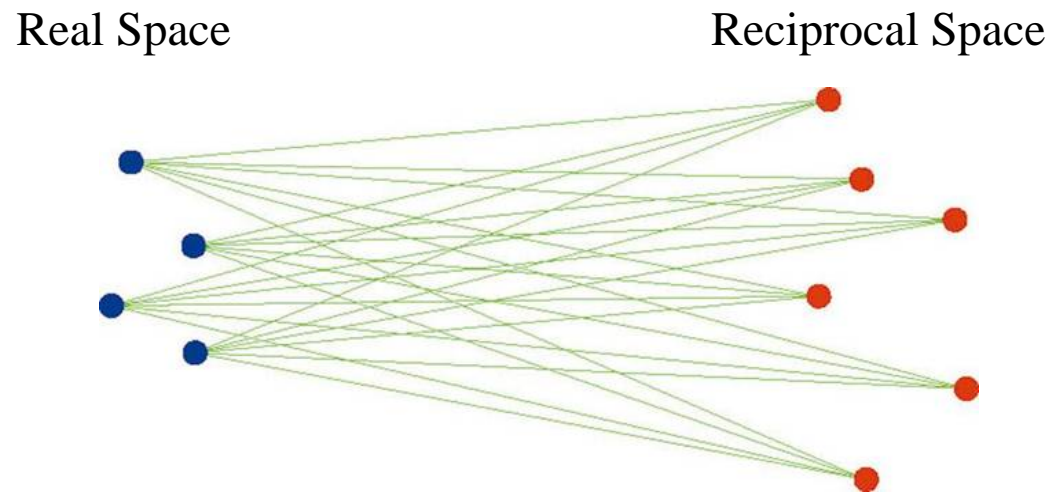
Jiang, Song, Chen, Xu, Raines, Fahimian, Lu, Lee, Nakashima, Urano, Ishikawa, Tamanoi & Miao, *PNAS* **107**, 11234 (2010).

Ankylography and Super-Resolution Crystallography

Ankylography: Derived from Greek words *ankylos* - ‘curved’ and *graphein* - ‘writing’.

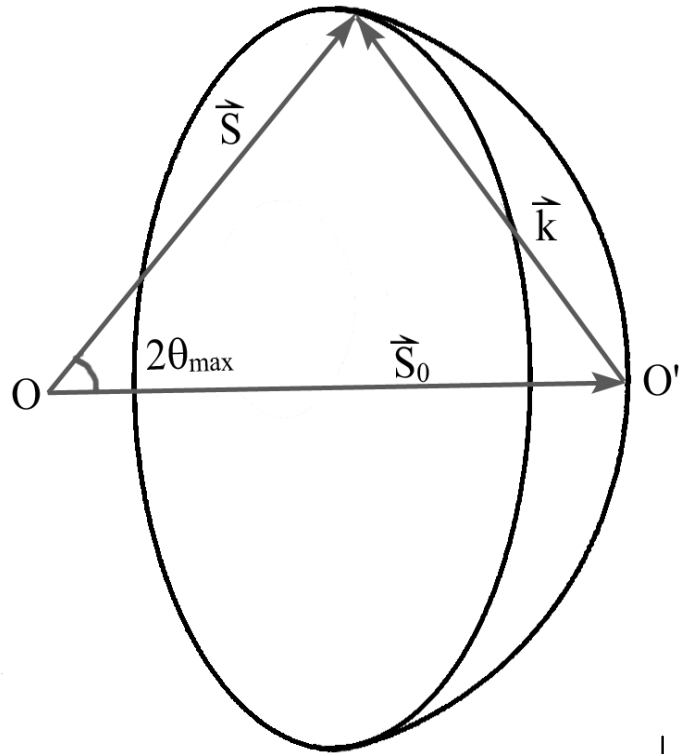
Raines, Salha, Sandberg, Jiang, Rodríguez, Fahimian, Kapteyn, Du, Miao, *Nature* **463**, 214-217 (2010).

Super-resolution crystallography: Schroder, Levitt, Brunger, Super-resolution biomolecular crystallography with low-resolution data, *Nature* **464**, 1218-1222 (2010).



Personnel view: the way of our thinking should not be confined with the Fourier transform.

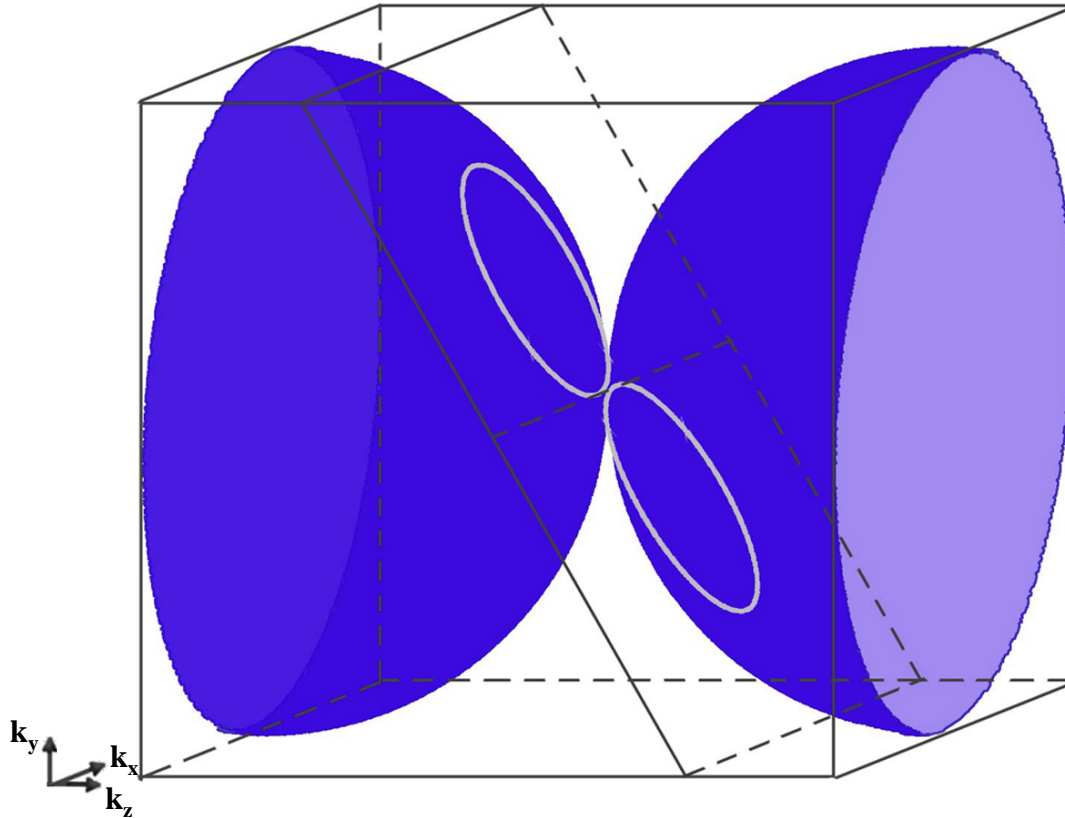
Oversampling of the Diffraction pattern on an Ewald Sphere Shell



$$|F(\theta, \varphi)| = \left| \int_V \rho(\vec{r}) e^{-\frac{2\pi i}{\lambda} [x \sin \theta \cos \varphi + y \sin \theta \sin \varphi + z(\cos \theta - 1)]} d^3\vec{r} \right|$$

O_d : The ratio of the number of non-centro-symmetrical intensity points on the Ewald sphere to the number of voxels sampling an object.

Oversampled Spherical Diffraction Pattern \Rightarrow All Possible Sample Orientations



The oversampled diffraction intensities on an Ewald sphere shell form a set of the intersected arcs, circles and point in *all possible* orientations of a 3D sample.

Considering a 3D Object and Phases as Unknown Variables

$$\begin{aligned} F(k_x, k_y, k_z) &= A_{k_x, k_y, k_z} \exp(i\phi_{k_x, k_y, k_z}) \\ &= \sum_{x, y, z=-M}^M \rho(x, y, z) \exp\left[\frac{-2\pi i(k_x x + k_y y + k_z z)}{2N + 1}\right] \end{aligned}$$

$$\begin{aligned} A_{k_x, k_y, k_z} \cos(\phi_{k_x, k_y, k_z}) &= \sum_{x, y, z=-M}^M \rho(x, y, z) \cos\left[\frac{2\pi i(k_x x + k_y y + k_z z)}{2N + 1}\right] \\ A_{k_x, k_y, k_z} \sin(\phi_{k_x, k_y, k_z}) &= - \sum_{x, y, z=-M}^M \rho(x, y, z) \sin\left[\frac{2\pi i(k_x x + k_y y + k_z z)}{2N + 1}\right] \end{aligned}$$

$$\forall k_x, k_y, k_z : k_x^2 + k_y^2 + (k_z + N)^2 = N^2$$

Matrix Representation of the Oversampled Intensities on an Ewald Sphere Shell

$$A = BX$$

$$A = \begin{pmatrix} A_1 \cos(\phi_1) \\ \vdots \\ A_L \cos(\phi_L) \\ A_0 \\ A_1 \sin(\phi_1) \\ \vdots \\ A_L \sin(\phi_L) \end{pmatrix} \quad B = \begin{pmatrix} \cos\left[\frac{2\pi(k_{x1}x_{-M} + k_{y1}y_{-M} + k_{z1}z_{-M})}{2N+1}\right] & \cdots & \cos\left[\frac{2\pi(k_{x1}x_M + k_{y1}y_M + k_{z1}z_M)}{2N+1}\right] \\ \vdots & \vdots & \vdots \\ \cos\left[\frac{2\pi(k_{xL}x_{-M} + k_{yL}y_{-M} + k_{zL}z_{-M})}{2N+1}\right] & \cdots & \cos\left[\frac{2\pi(k_{xL}x_M + k_{yL}y_M + k_{zL}z_M)}{2N+1}\right] \\ 1 & \cdots & 1 \\ -\sin\left[\frac{2\pi(k_{x1}x_{-M} + k_{y1}y_{-M} + k_{z1}z_{-M})}{2N+1}\right] & \cdots & -\sin\left[\frac{2\pi(k_{x1}x_M + k_{y1}y_M + k_{z1}z_M)}{2N+1}\right] \\ \vdots & \vdots & \vdots \\ -\sin\left[\frac{2\pi(k_{xL}x_{-M} + k_{yL}y_{-M} + k_{zL}z_{-M})}{2N+1}\right] & \cdots & -\sin\left[\frac{2\pi(k_{xL}x_M + k_{yL}y_M + k_{zL}z_M)}{2N+1}\right] \end{pmatrix}$$

$$X = \begin{pmatrix} \rho(x_{-M}, y_{-M}, z_{-M}) \\ \vdots \\ \rho(x_M, y_M, z_M) \end{pmatrix} \quad \forall k_{xi}, k_{yj}, k_{zk} : \left(N - \frac{1}{2}\right)^2 \leq k_{xi}^2 + k_{yj}^2 + (k_{zk} + N)^2 < \left(N + \frac{1}{2}\right)^2$$

Making B a Square Matrix by Padding Zeros around the Object

$$B' = \begin{pmatrix} \cos\left[\frac{2\pi(k_{x1}x_{-L} + k_{y1}y_{-L} + k_{z1}z_{-L})}{2N+1}\right] & \dots & \dots & \cos\left[\frac{2\pi(k_{x1}x_L + k_{y1}y_L + k_{z1}z_L)}{2N+1}\right] \\ \vdots & & & \vdots \\ -\sin\left[\frac{2\pi(k_{xL}x_{-L} + k_{yL}y_{-L} + k_{zL}z_{-L})}{2N+1}\right] & \dots & \dots & -\sin\left[\frac{2\pi(k_{xL}x_L + k_{yL}y_L + k_{zL}z_L)}{2N+1}\right] \end{pmatrix} \quad B$$

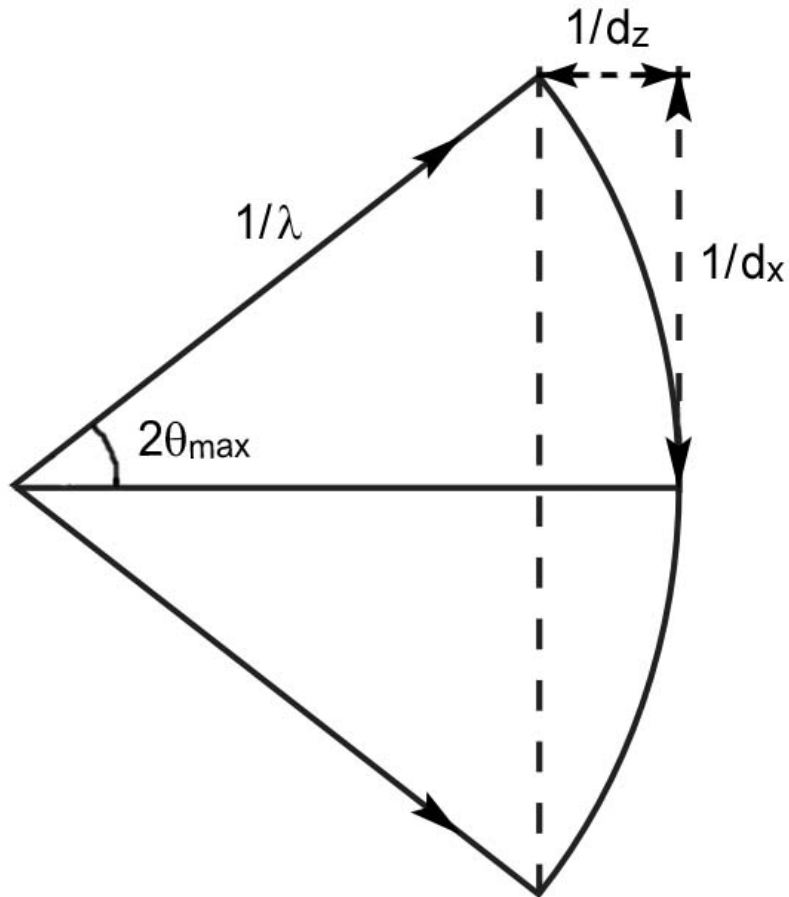
$$X' = \begin{pmatrix} 0 \\ \vdots \\ 0 \\ X \\ 0 \\ \vdots \\ 0 \end{pmatrix}$$

$$B' X' = A$$

For small objects, the rank of $B' >$ the number of unknown variables.

For larger objects, extra real-space constraints are needed to reduce the # of unknown variables.

3D Spatial Resolution in Ankylography

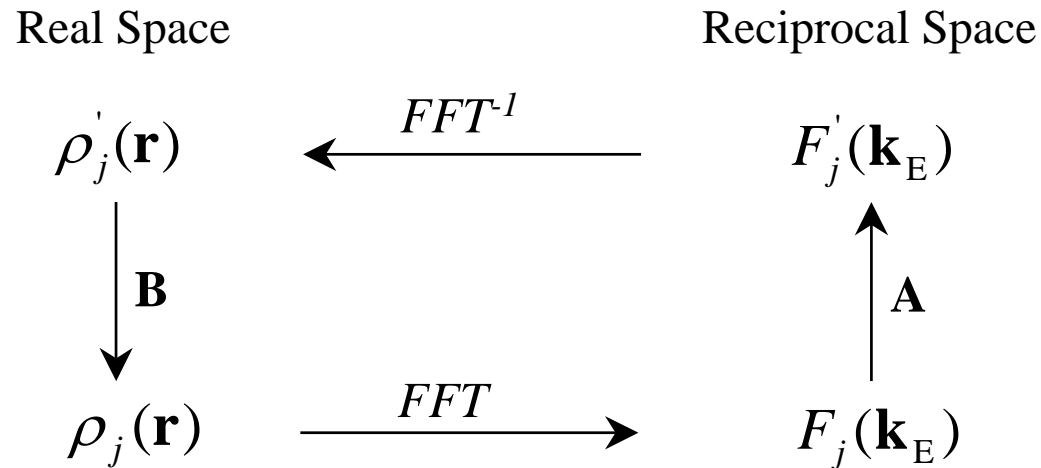


$$d_x = d_y = \frac{\lambda}{\sin(2\theta_{\max})}$$

$$d_z = \frac{\lambda}{2\sin^2 \theta_{\max}}$$

Paraxial approximation ($\sin \theta \approx \theta$) is assumed in Fresnel and Fraunhofer diffraction, but not in Ankylography.

Ankylographic Reconstruction



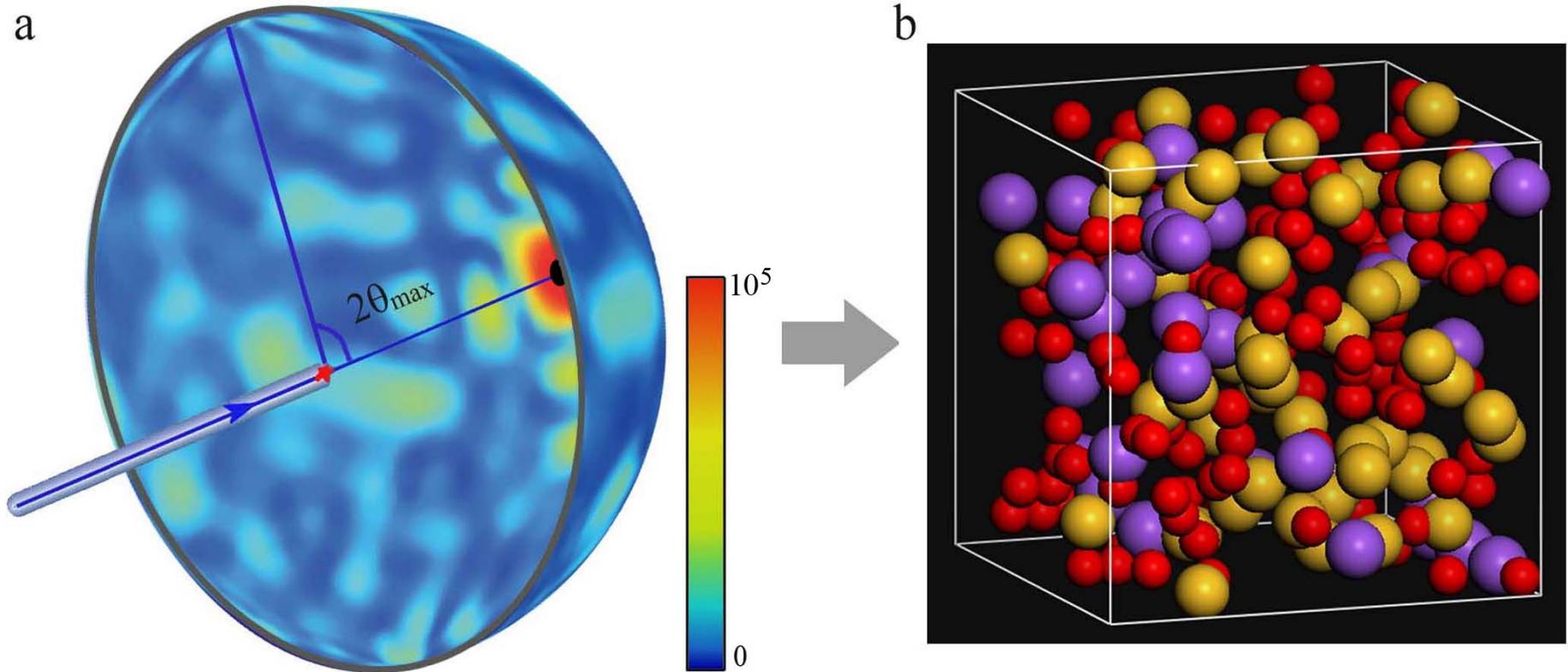
Real-Space Constraints:

- (i) Optimization of the random initial phase set.
- (ii) Uniformity outside the support.
- (iii) Positivity and continuity inside the support.
- (iv) Amplitude extension^{1,2}.
- (v) More possible constraints: atomicity, histogram matching, bond distance and angles, molecular replacement, noncrystallographic symmetry

¹Raines, Salha, Sandberg, Jiang, Rodríguez, Fahimian, Kapteyn, Du, Miao, *Nature* **463**, 214-217 (2010).

²Schroder, Levitt, Brunger, Super-resolution biomolecular crystallography with low-resolution data, *Nature* **464**, 1218-1222 (2010).

3D Structure Determination of a Sodium Silicate Glass Particle from a Simulated and Noisy 2D Spherical Diffraction Pattern Alone



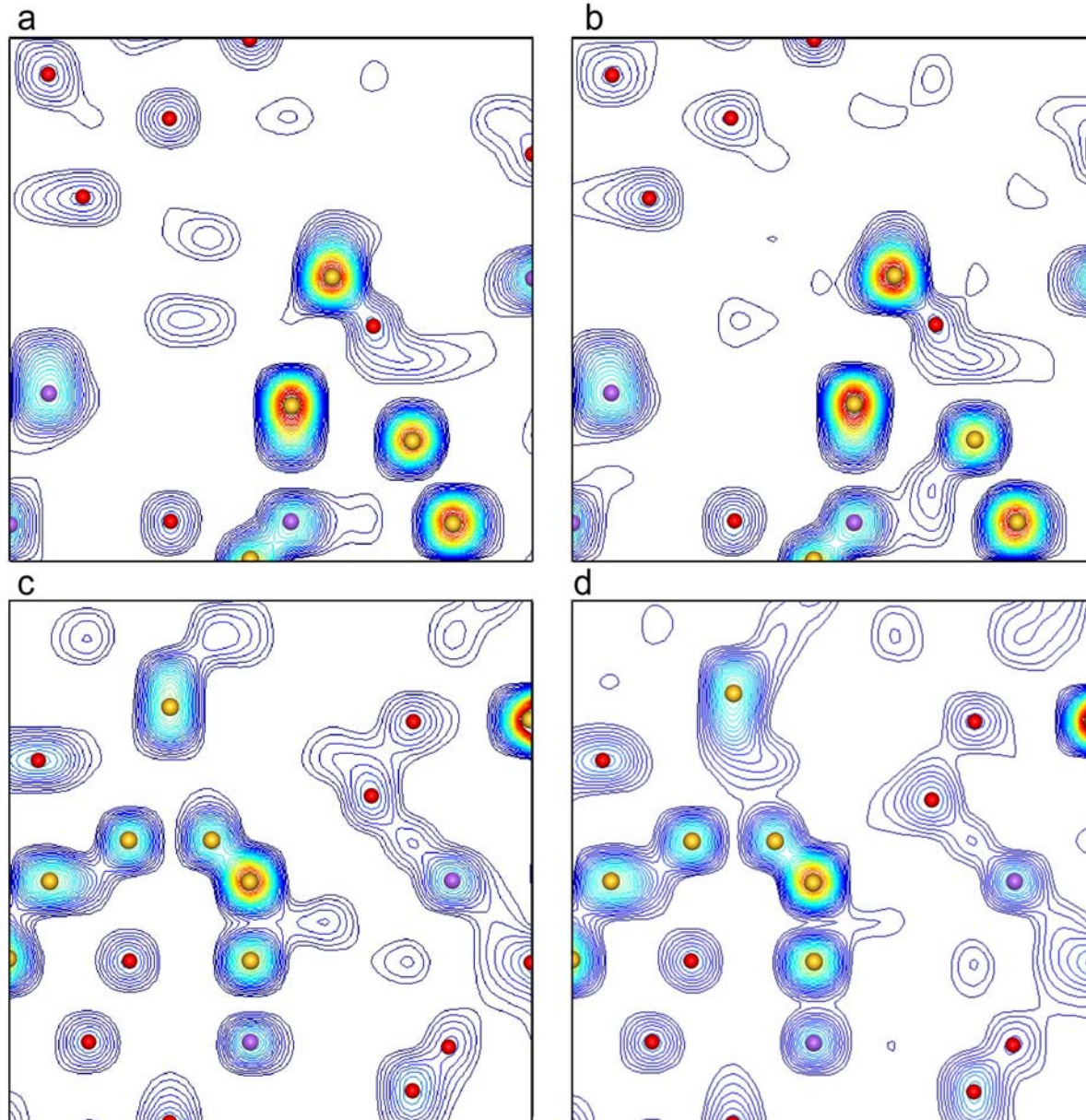
Particle Size: $14 \times 14 \times 14 \text{ \AA}^3$
 $2\theta_{\max} = 90^\circ$
Sample array: 14^3 voxels

$\lambda = 2 \text{ \AA}$
 $d_x = d_y = d_z = 2 \text{ \AA}$

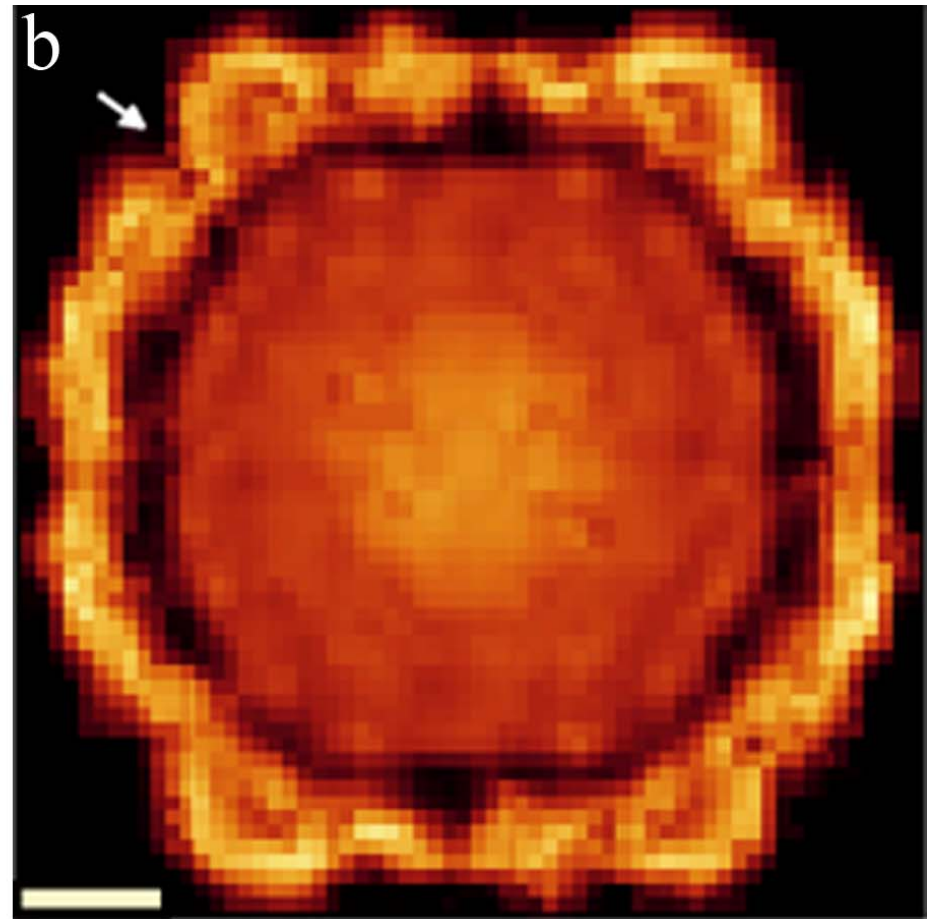
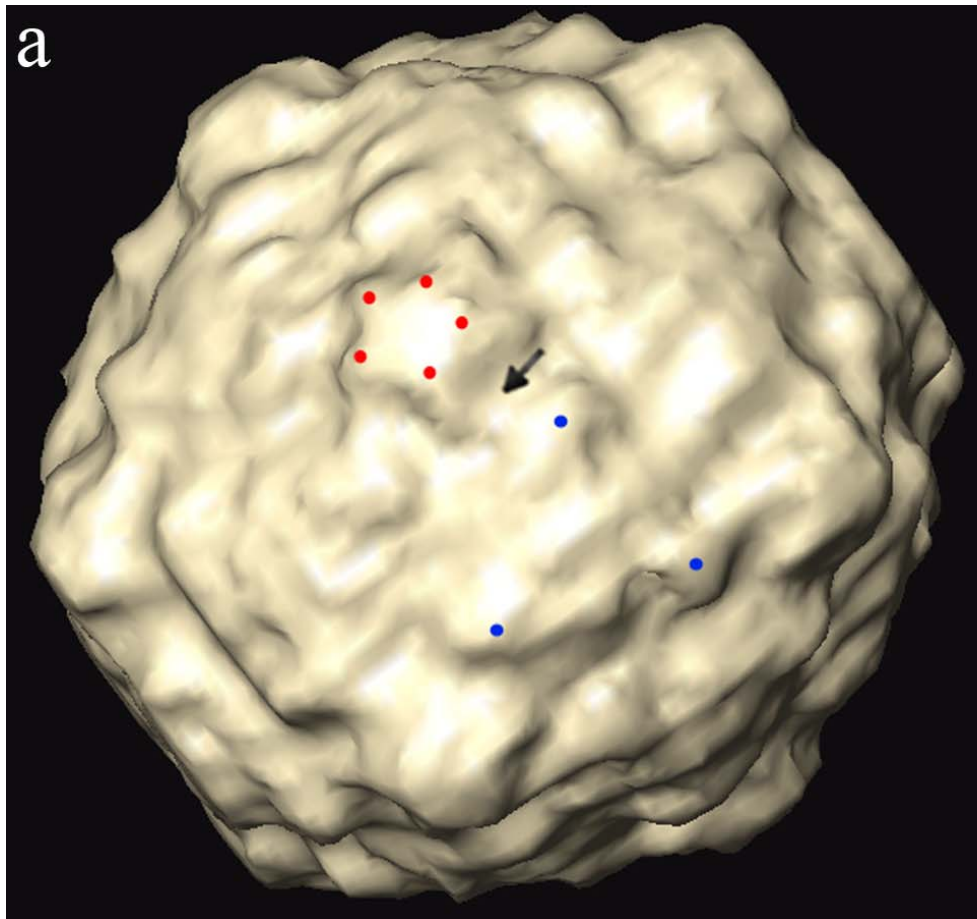
Red, purple and yellow: O, Na and Si atoms

Incident flux = 10^{13} photons
Poisson noise added
Fourier-space array: 64^3 voxels

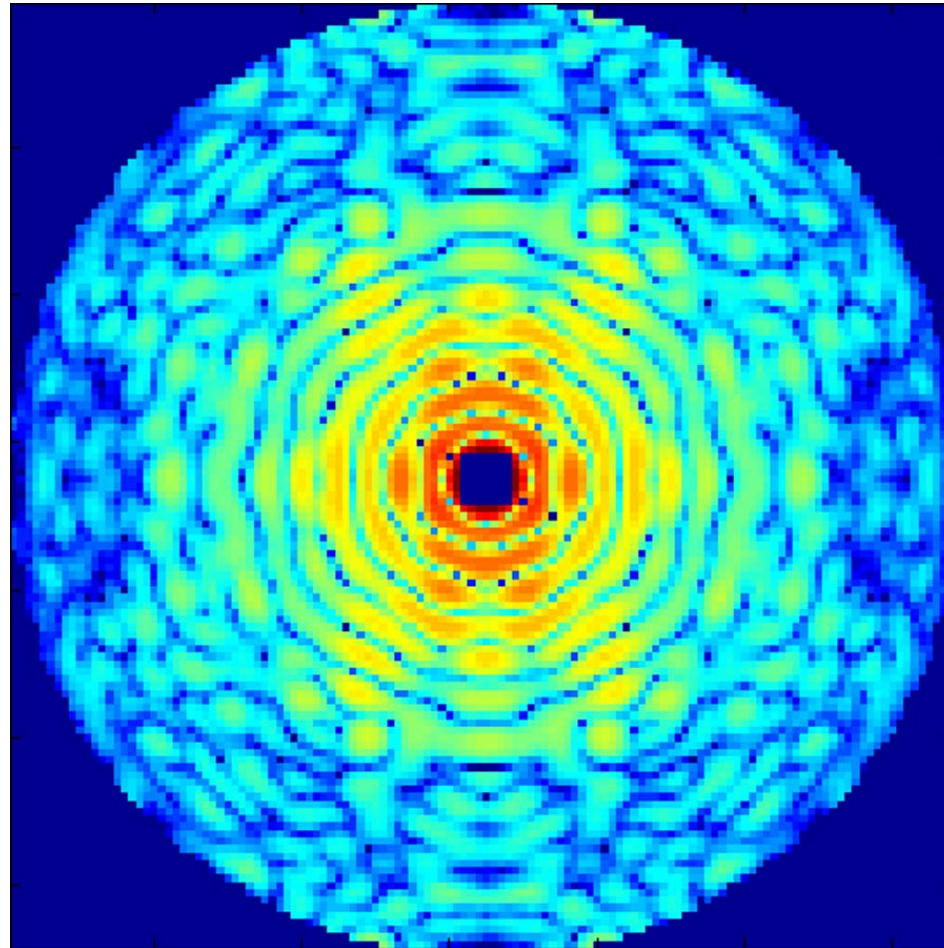
Two Perpendicular Slices of the Reconstructed Sodium Silicate Glass Particle



3D Structure of a Poliovirus Displayed at 2 – 3 nm Resolution



Simulated 2D Spherical Diff. Pattern of an Individual Poliovirus from a Single X-FEL Pulse



$\lambda = 1.77$ nm

Flux = 10^{13} photons

Focal spot: 100 nm

Poisson noise added

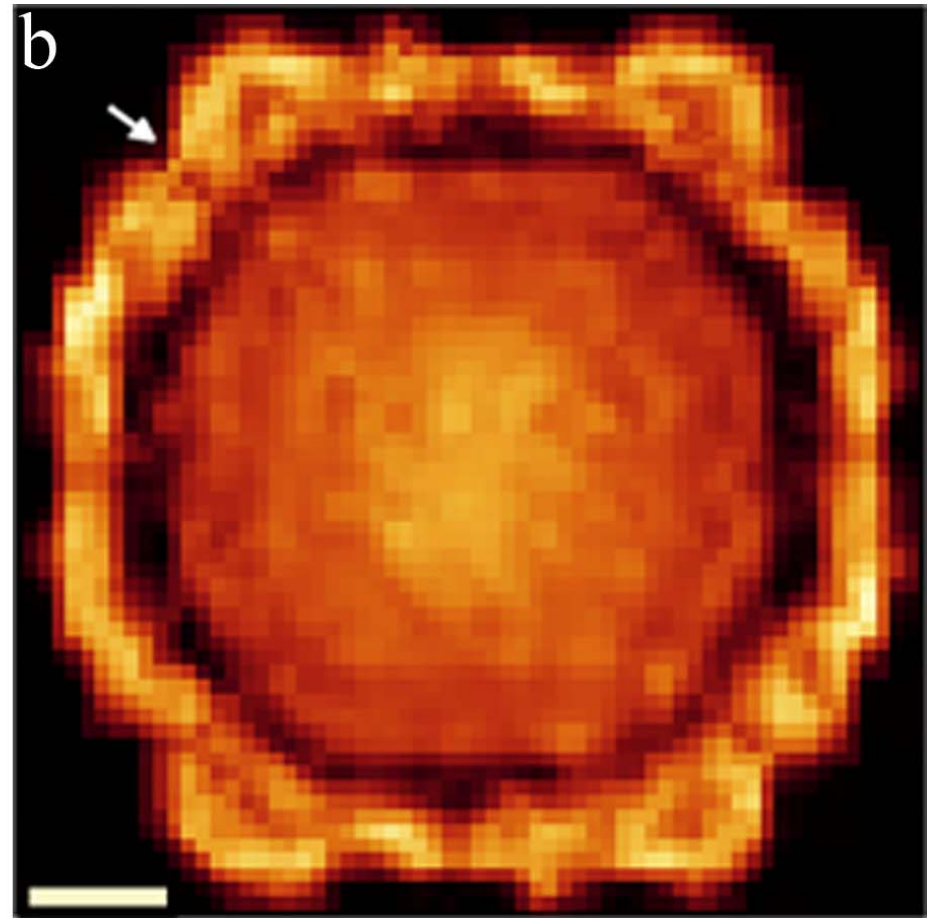
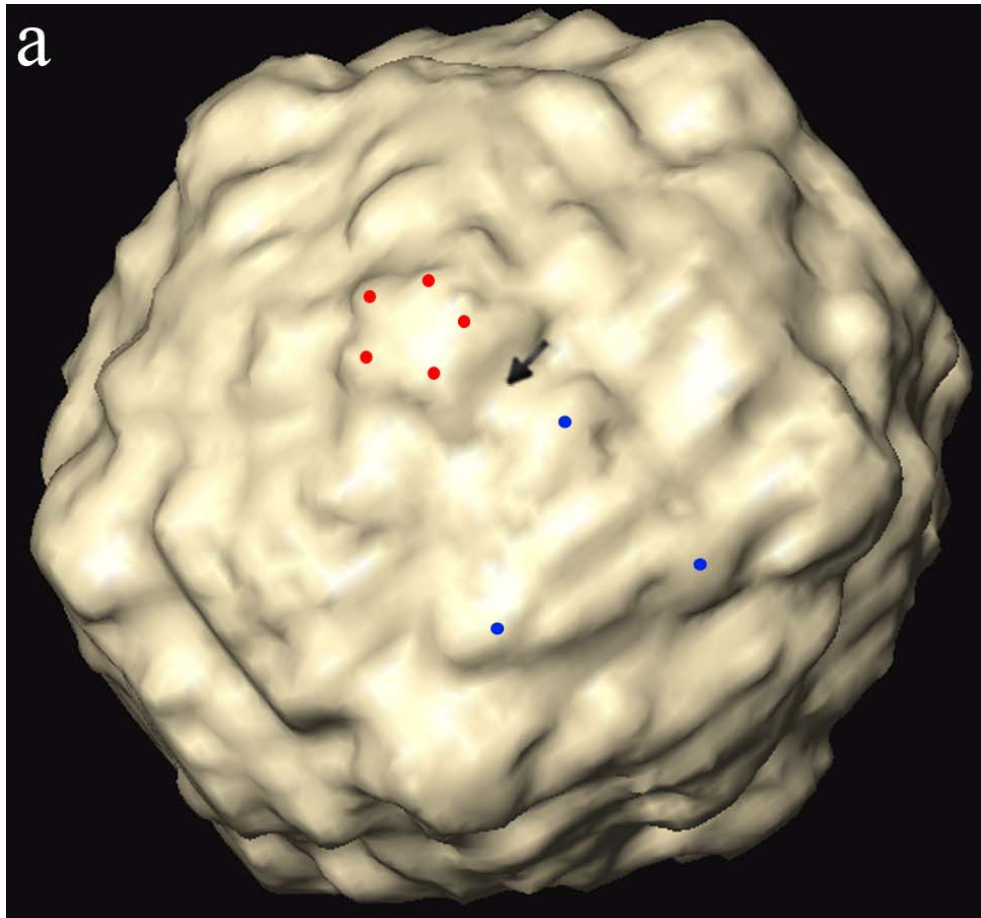
$2\theta_{\max} = 62.7^\circ$

$d_x = d_y = 2$ nm and $d_z = 3.3$ nm

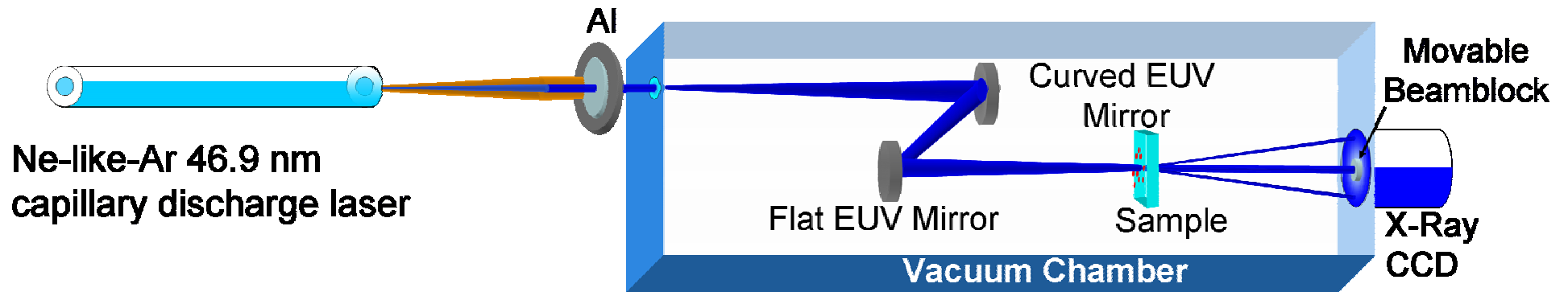
Sample array: $32 \times 32 \times 20$ voxels

Fourier-space array: $128 \times 128 \times 78$ voxels

3D Structure Determination of the Poliovirus from a Single Simulated X-FEL Pulse



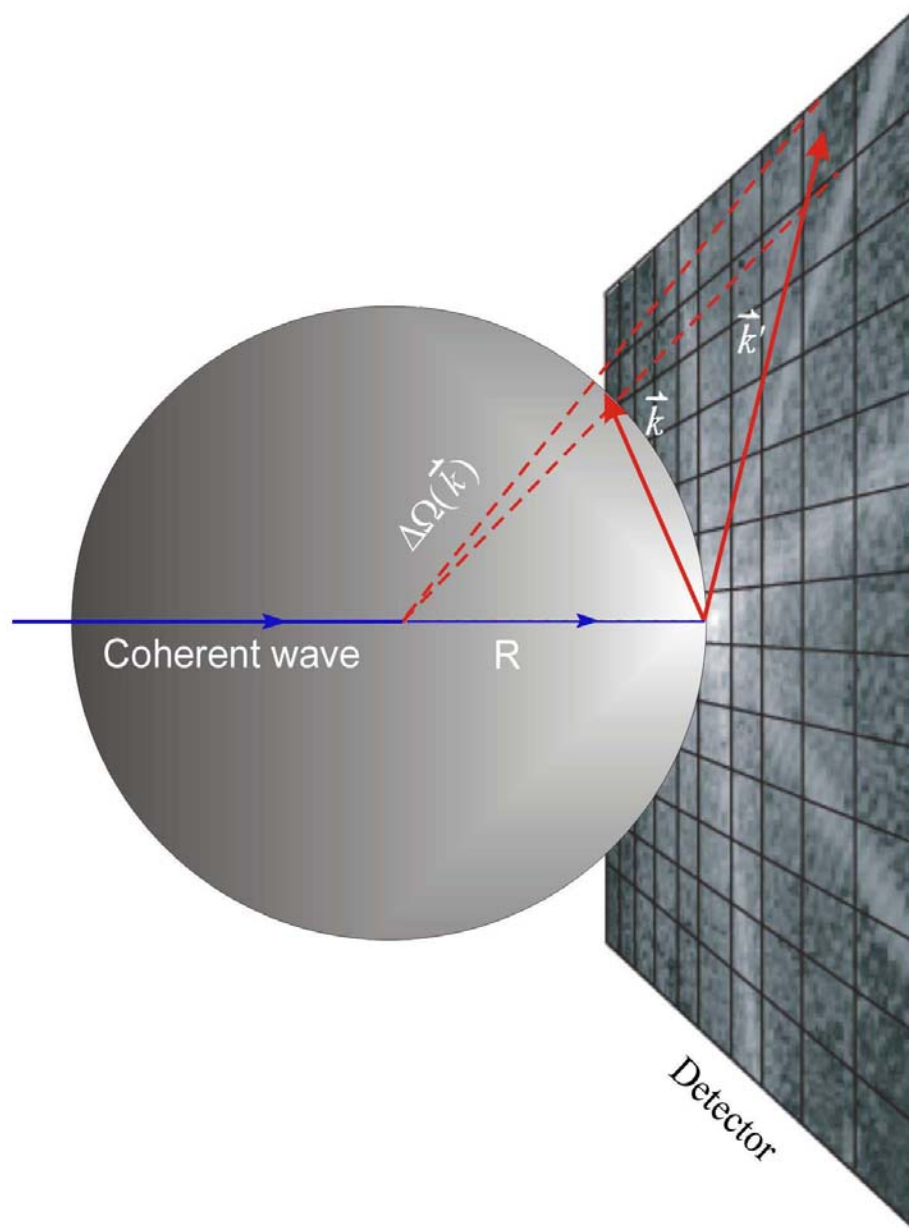
Soft X-ray Laser Used for Experimental Demonstration of Ankylography



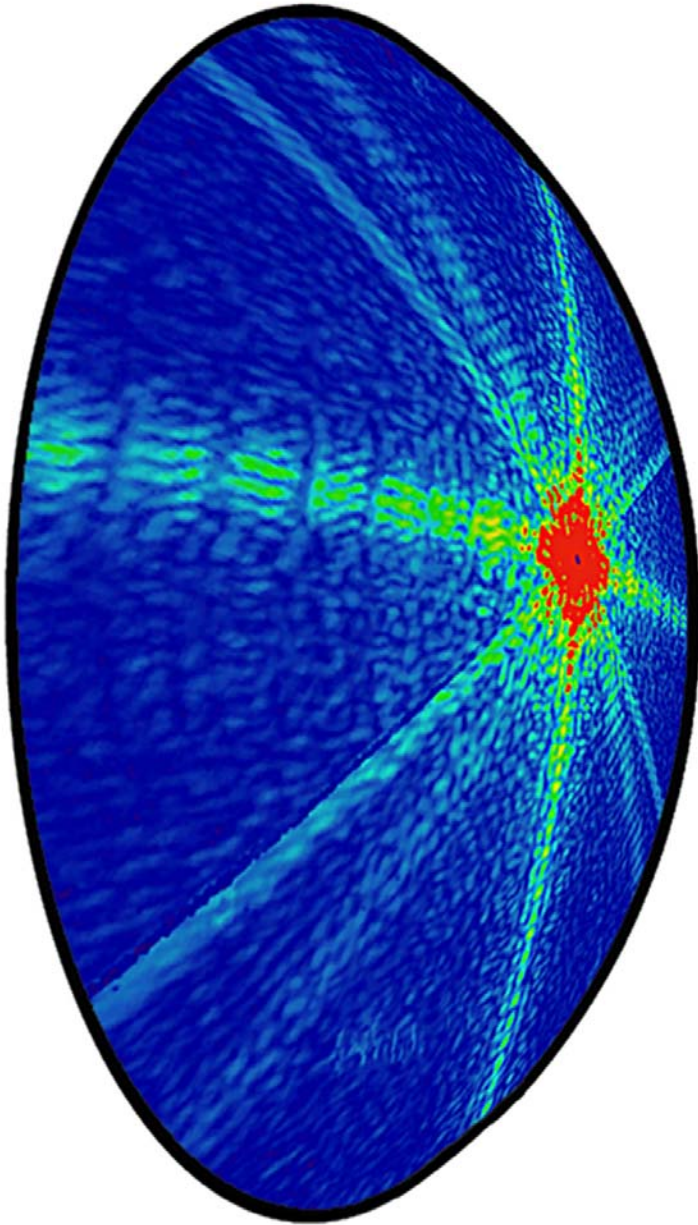
$$\lambda = 46.9 \text{ nm} \quad \lambda / \Delta\lambda = 10^4$$

Andor CCD detector (2048×2048 pixels, 13.5 μm×13.5 μm pixel size).

Projection of an Oversampled 2D Diff. Pattern from a Planar Detector onto the Ewald Sphere



Oversampled Diffraction Pattern of a Test Specimen on the Ewald Sphere



420×420×240 voxels

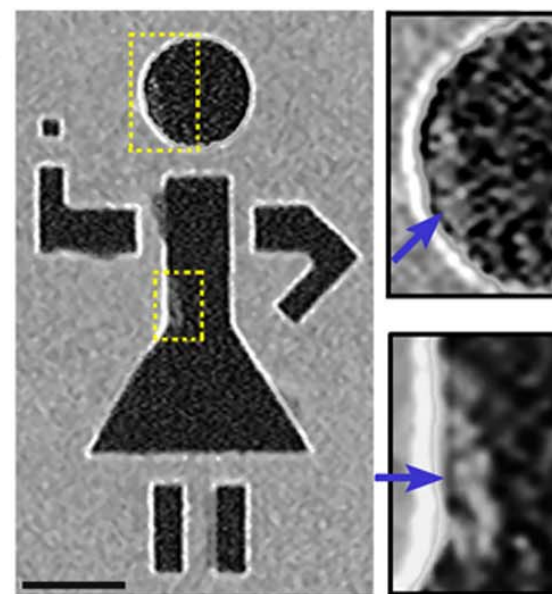
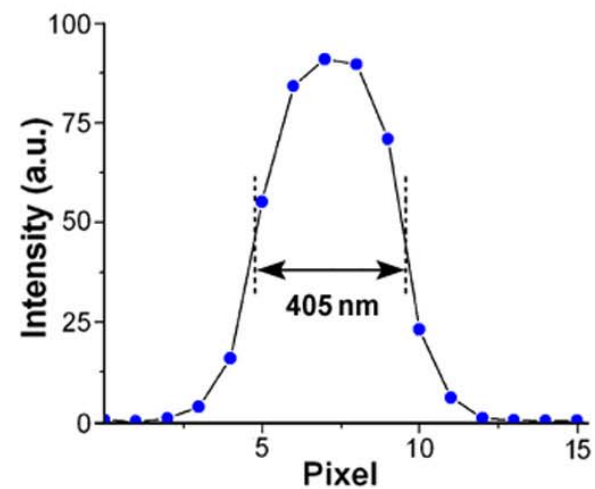
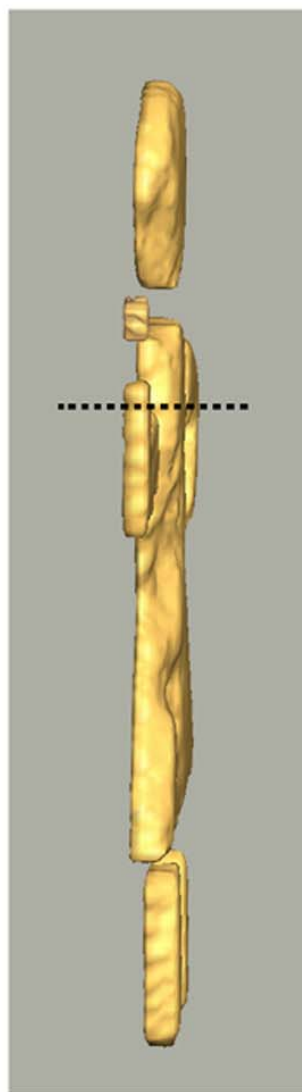
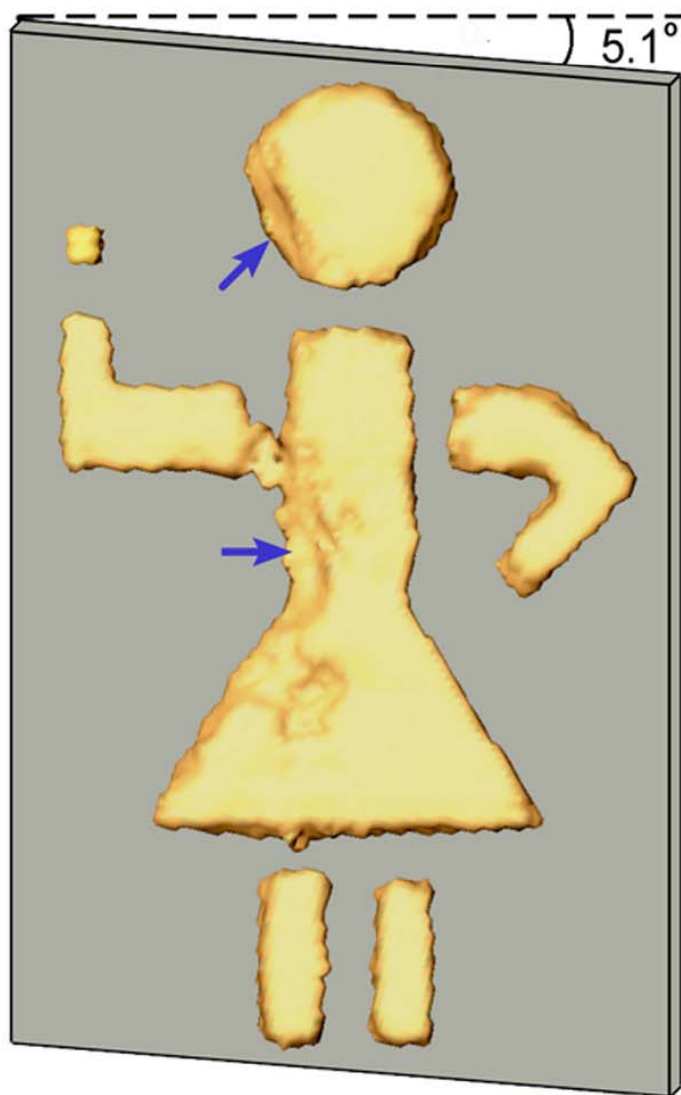
$O_d = 2.6$

Diffraction angle at the corner: 48.3°

Diffraction angle at the edge: 35.9°

Reconstruction error R-factor : 8%

Demonstration of Ankylography Using Experimental Data Obtained with the Soft X-ray Laser



Summary

- Oversampled diff. pattern on an Ewald sphere shell \Rightarrow 3D structure information.
- 3D structure determination of a sodium silicate glass particle at 2 Å resolution from a simulated 2D spherical diffraction pattern alone.
- 3D structure determination of an individual poliovirus from a single simulated X-FEL pulse.
- Demonstration of ankylography using experimental data obtained with a soft X-ray laser.
- Ankylography – Science of Cubism?

Collaborators

JILA & U. Colorado, Boulder

*Richard Sandberg, Henry Kapteyn,
Margaret Murnane*

RIKEN/SPring-8

Changyong Song, Tetsuya Ishikawa

University of North Texas

Jincheng Du

LBNL

Anne Sakdinawat

Colorado State University

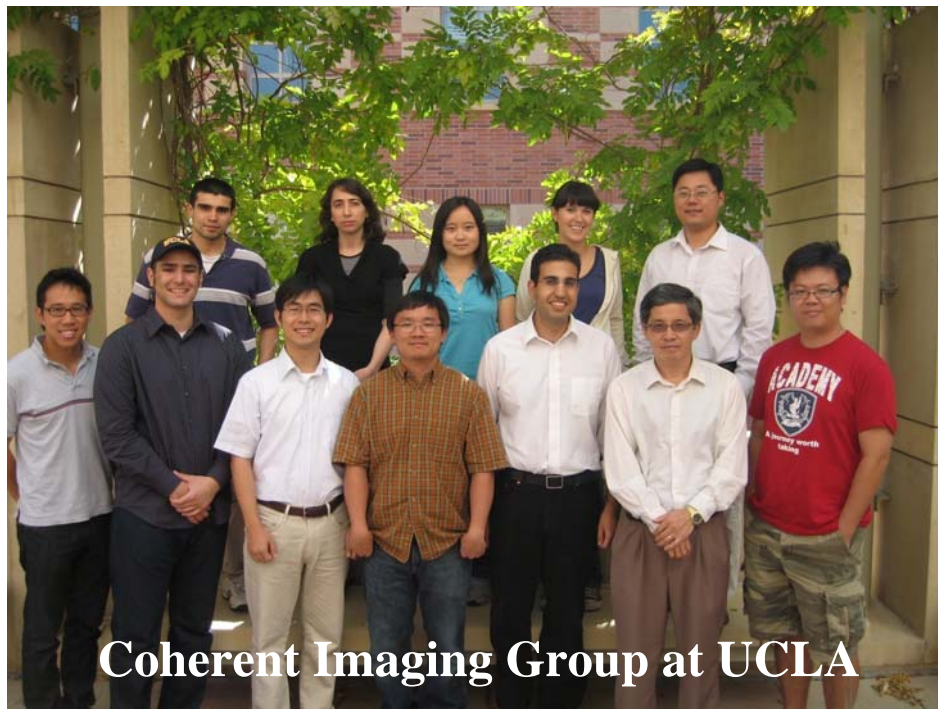
Jorge Rocca's group

UCLA Medical School

Fuyu Tamanoi

Academia Sinica, Taiwan

T.-K. Lee



Coherent Imaging Group at UCLA